

1 **Supplemental methods and materials: The genomic consequences and**
2 **persistence of sociality in spiders**

3
4 Jilong Ma^{1,2*}, Jesper Bechsgaard², Anne Aagaard², Palle Villesen¹, Trine Bilde^{2*§}, Mikkel Heide
5 Schierup^{2*§}

6
7 1. Bioinformatics Research Centre, Aarhus University, DK-8000 Aarhus C, Denmark
8 2. Department of Biology, Aarhus University, DK-8000 Aarhus C, Denmark

9
10 * Corresponding authors: aujilongm@birc.au.dk, trine.bilde@bio.au.dk, mheide@birc.au.dk

11 \$ shared last authorship

12
13
14

Section 1 - Sampling and Sequencing

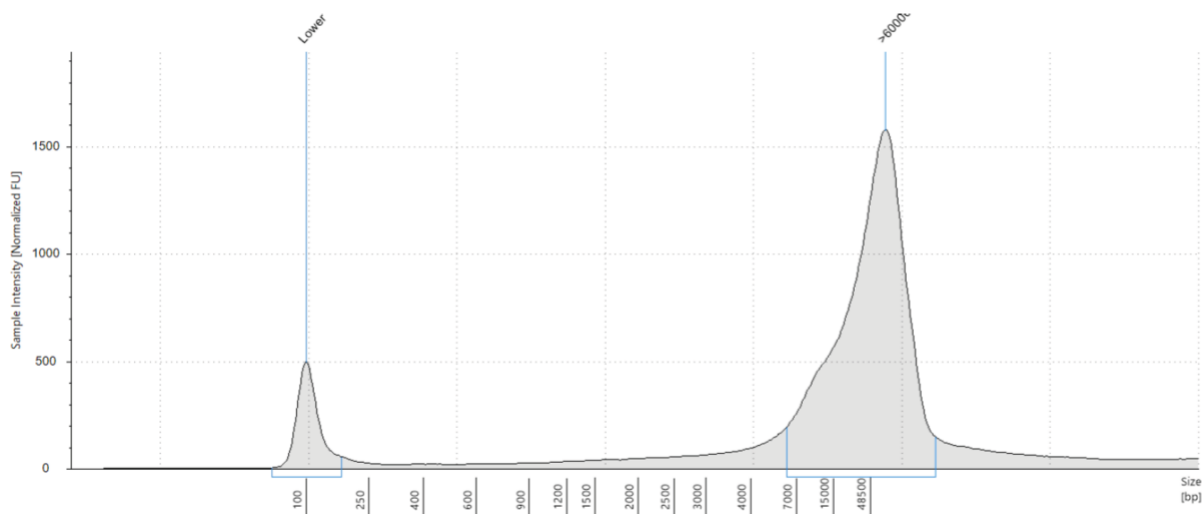
15 DNA - long reads

16 A single individual from *S. dumicola* (Namibia - Otavi), *S. tentoriicola* (South Africa - Tierberg), *S.*
17 *mimosarum* (South Africa - Weenen), *S. sarasinorum* (India - Unknown), *S. bicolor* (Namibia - Betta)
18 and *S. lineatus* (Israel - Negev Desert) were sampled, and DNA was extracted using the MagAttract
19 HWM DNA kit from Qiagen (Hilden, Germany). The DNA was fragmented to 15-20 kb fragments
20 using Megaruptor 3, and libraries were prepared using Pacific Biosciences protocol for HiFi library
21 prep using SMRTbell® ExpressTemplate Prep Kit 3.0. Final library was size selected using
22 BluePippin with a 10kb cut-off. Each library was sequenced on three 8M SMRT cells on Sequel II
23 instrument using Sequel II Binding kit 2.2 and Sequencing chemistry v2.0. Loading was performed by
24 adaptive loading, movie time: 30 hours, pre-extension: 2 hours. Between 66 and 99 gb data was
25 obtained (see Supplementary Table S1).

26 Tapestation profiles of DNA extractions for long read sequencing:

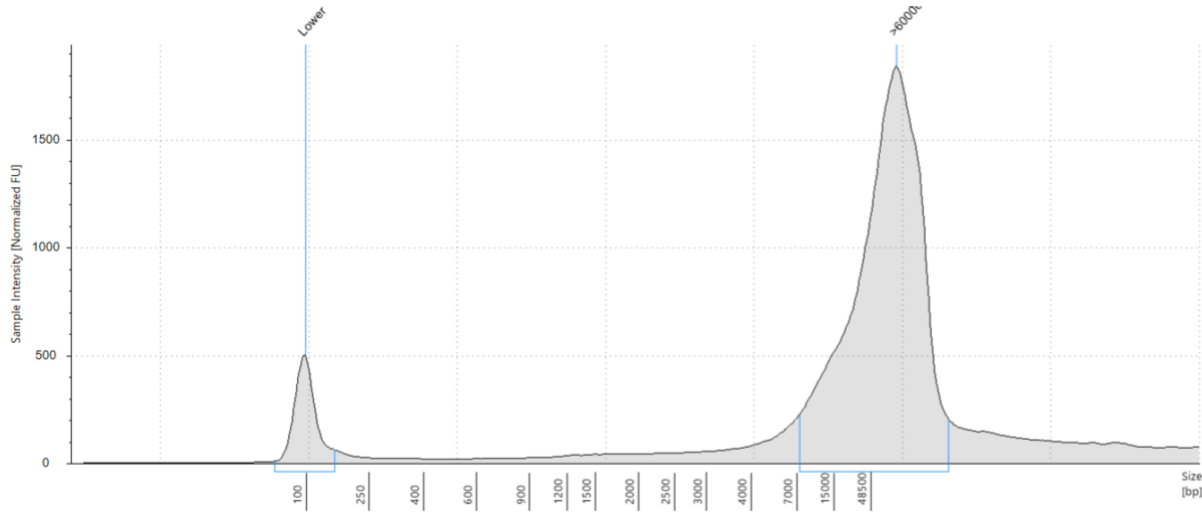
27 Electropherogram of DNA used for PacBio HiFi sequencing on an Agilent TapeStation for each of the
28 six species. The peak around 100bp serves as a standard for both fragment size and intensity.

29 *Stegodyphus dumicola*:



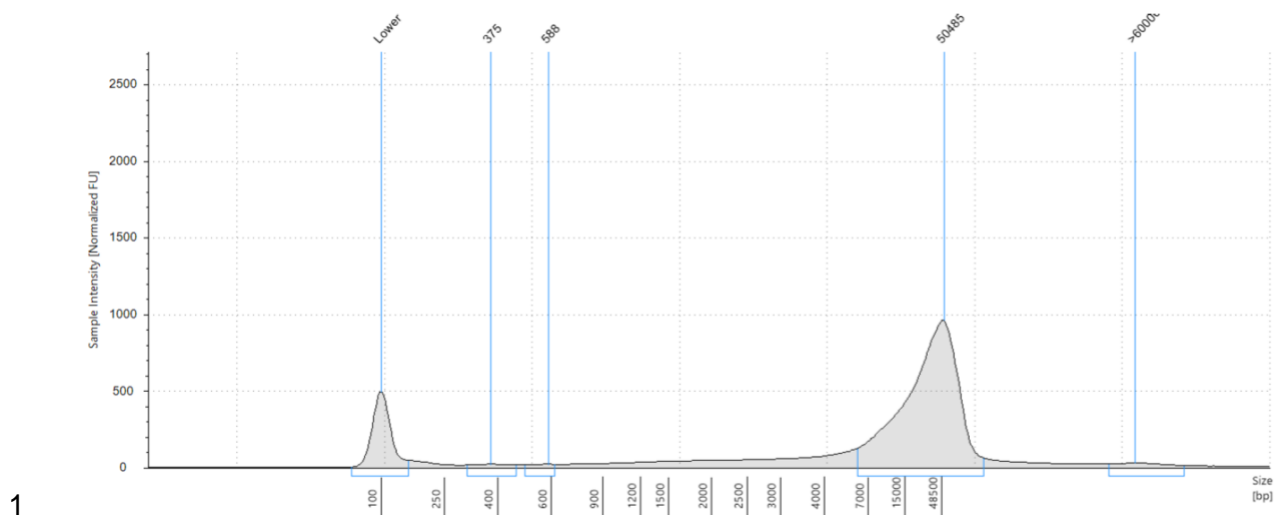
1

2 *Stegodyphus tentoriicola*:

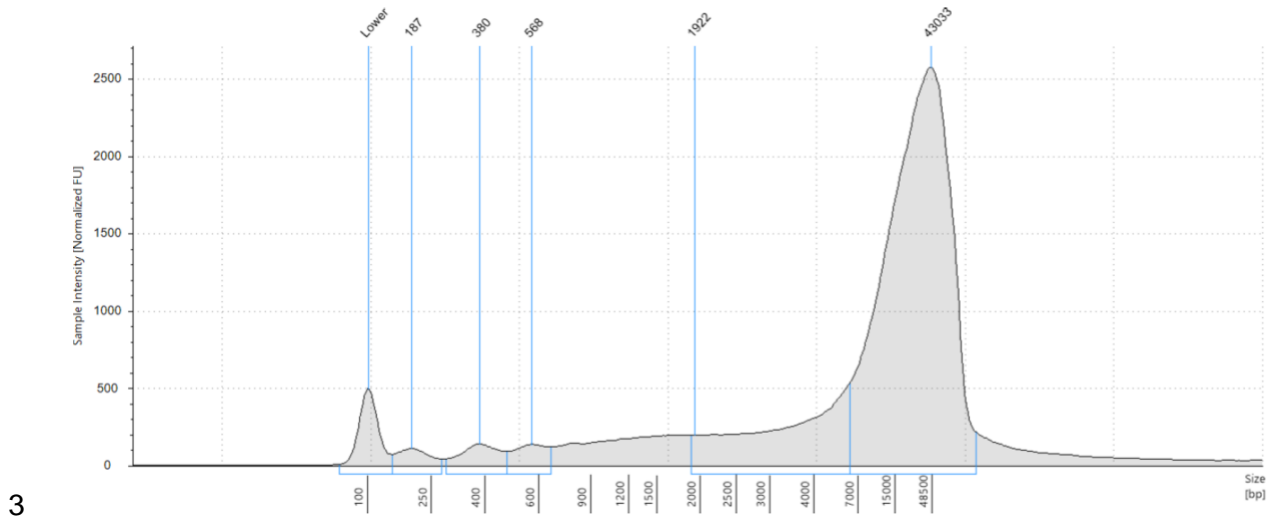


3

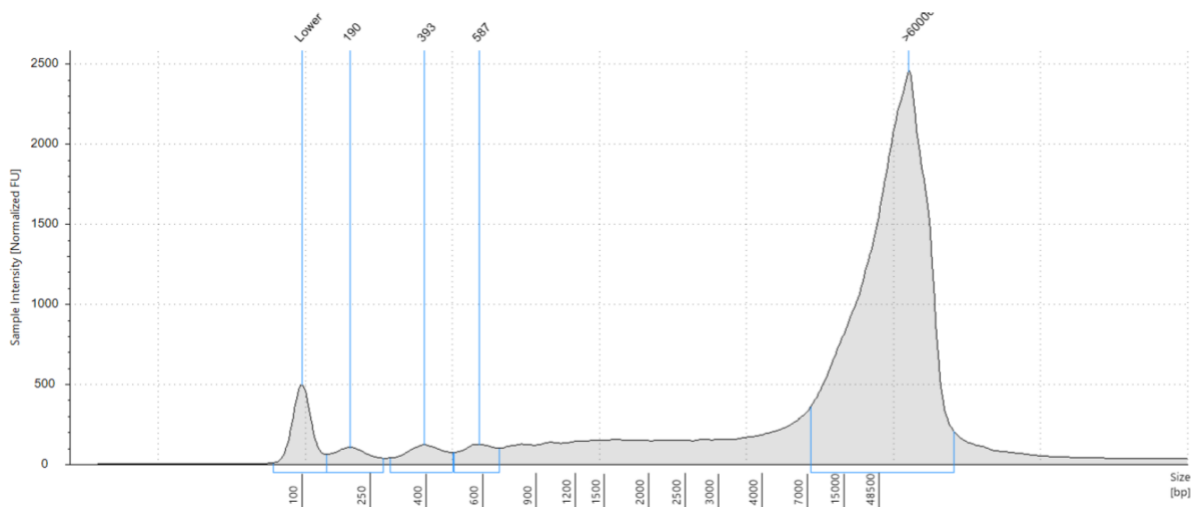
4 *Stegodyphus mimosarum*:



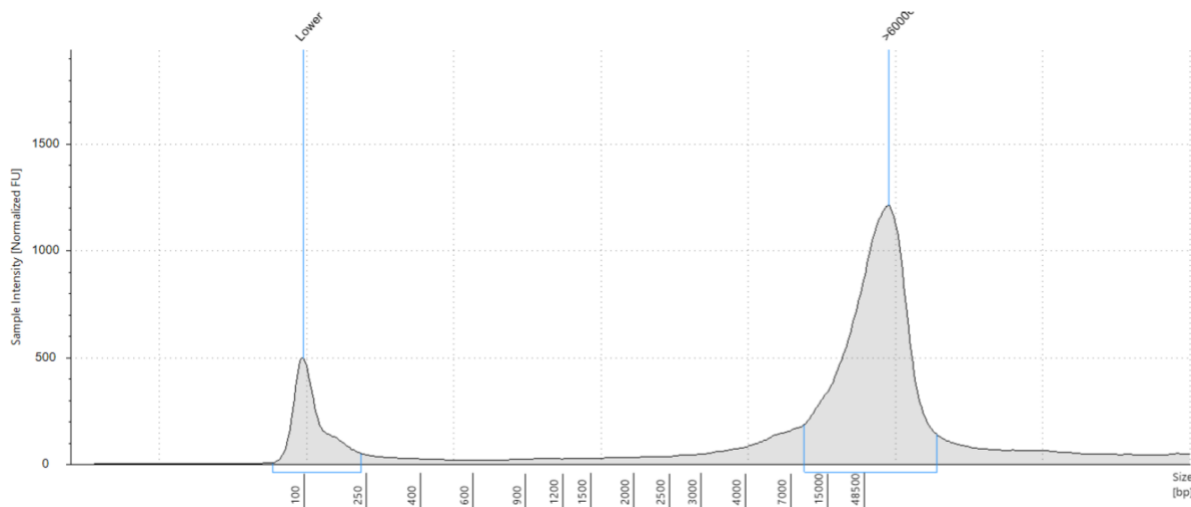
2 *Stegodyphus sarasinorum*:



4 *Stegodyphus bicolor*:



2 *Stegodyphus lineatus*:



4 DNA - Hi-C

5 A single individual from each species from the same populations that were sampled for PacBio
 6 sequencing were sampled for hi-C sequencing. The social individuals were taken from the same nests.
 7 Libraries were prepared from 6 legs per species using the Dovetail® Omni-C® Kit, and each library
 8 was sequenced using DNBSEQ-G400 to obtain between 139 and 153 gb 150PE data per sample (see
 9 Supplementary Table S1).

10

1 Resequencing

2 From each of the social species two individuals from isolated genetic lineages were sampled for
3 resequencing to use for estimating ‘social’ d_N/d_S ratios (π_N/π_S in practice). From *S. mimosarum*,
4 individuals were sampled in South Africa (Weenen) and Madagascar (Antananarivo); from *S.*
5 *dumicola*, individuals were sampled from two populations in Namibia (Otavi and Betta); from *S.*
6 *sarasinorum*, individuals were sampled from Himalaya and Sri Lanka (Settepani et al. 2014). Five
7 single individuals from the subsocial *S. pacificus* were sampled in India for resequencing to be used
8 for generating a reference genome by aligning reads to chromosome-level assembly of *S.*
9 *sarasinorum*. DNA from all individuals were extracted using the Qiagen Blood and Tissue kit, Qiagen
10 (Hilden, Germany), and the DNA was sequenced using DNBSEQ-G400 to obtain at between 40 and
11 146 gb 150PE data per sample (see Supplementary Table S1). DNBSEQ is a high-throughput DNA
12 sequence technology developed in BGI. Its quality score per nucleotide per read would be lower than
13 HiFi. Nevertheless, our individuals have a decent coverage depth per genome to call and filter for
14 solid variants. Hence, the final variant quality from short read sequencing (π_N/π_S) and HiFi
15 genomes (d_N/d_S) would be comparable. We are confident that technology differences would not raise
16 noise that heavily biased the comparison of results.

17

18 RNA resequencing

19 To guide the annotation of protein-coding genes, we sequenced the transcriptomes of several
20 individuals from each species. Three to five families were established by controlled crosses, and three
21 offspring from each family were sampled as spiderlings (n=3), subadults (n=3) and adults (n=3). All
22 parental individuals came from the same populations as used for long read and Hi-C sequencing.
23 Families were produced as follows: 1) Social species were mated among individuals from the same
24 nest. Initially we created several groups (15+) of 6 subadults to be sure they were virgins until we
25 could determine the sex. When they became adults, we kept only groups with 1 male and 5 females. A

1 few weeks after they were all sexually mature, we froze down the male, and placed the females in
2 individual boxes. The females that laid an egg sac were kept. After the eggs hatched and before
3 matriphagy, one female per group was frozen down and so were six of her offspring. 2) Subsocial
4 individuals were raised from hatching egg sacs produced by females collected in the wild. When
5 sexually mature, females and males with separate mothers were mated (15+), and the male was frozen
6 down. The females that laid an egg sac were kept. After the eggs hatched and before matriphagy, five
7 females were frozen down and so were six of their offspring.

8

9 We extracted RNA all individuals using the Qiagen RNeasy Mini kit, and sequencing libraries were
10 constructed using NEBNext Ultra II Directional RNA Library Prep Kit that were sequenced on
11 Illumina NovaSeq 6000 to obtain ~6GB 150PE data per individual. (see Supplementary Table S2)

12

13

14 Section 2 - *De novo* assemblies and annotations

15 **De novo assembly**

16 We generated chromosome-level assemblies for all six species with PacBio HiFi long reads and Hi-C
17 sequencing. We started with using Hifiasm(Cheng et al. 2021), a haplotype-resolved *de novo*
18 assembler for PacBio HiFi reads, to assemble contigs for each species using the default settings. Both
19 PacBio HiFi reads and Hi-C reads were used in this process. We then selected the haplotype with the
20 longer phased assembly graph to retrieve the fasta sequence for contig scaffolding.

21

22 Next, we used the Juicer software to align the Hi-C reads to the long read contigs generated in the
23 previous step. We subsequently employed the 3D-DNA (Dudchenko et al. 2017) run-asm-pipeline.sh
24 script to order and orient the contigs based on the aligned Hi-C reads. We customize the settings with
25 "-r 0 --editor-repeat-coverage 30 --editor-coarse-stringency 20" to omit mis-join correction rounds in
26 the 3D-DNA scaffolding pipeline. This decision was made because the mis-join correction tends to

1 break long contigs joined from PacBio HiFi long reads in our practice, which would introduce more
2 mis-joining. This customization resulted in a single "mega-scaffold" containing ordered and oriented
3 contigs, with 500 bp Ns introduced at the joints.

4

5 Finally, we examined the mega-scaffold Hi-C contact map to identify contigs belonging to the same
6 chromosome, as they exhibited distinct intra- and inter-chromosomal Hi-C contact patterns. We then
7 manually reviewed, edited, and split the mega-scaffold into chromosome-level scaffolds for each
8 species using Juicebox(Durand et al. 2016), ultimately generating the final chromosome-level fasta
9 file. The final Hi-C contact maps for all six species are shown in Figure S1. The Hi-C contact map
10 indicates that the scaffolding of chromosomes are visually clean with very few minor misjoined
11 contigs between chromosomes. Further manual curation on the HiC-scaffolding could have been
12 possible to "solve" the few seemingly mis-joints but we should claim clearly that there is no robust
13 way in confirming the precision of the manual curation result. The inherent characteristics of larger
14 contigs derived from long-read HiFi sequencing ensure that the credibility of subsequent analyses
15 focused on local variants and genes remains intact. This is due to the fact that potential local misjoins,
16 typically occurring at a broader spatial scale, do not significantly impact these analyses.

17

18 **Genome Annotations**

19 RepeatModeler2 (Flynn et al. 2020) was initially applied to construct repeat databases that are specific
20 to each species. Following this, we employed RepeatMasker (Tarailo-Graovac and Chen 2009) to
21 soft-mask the genome assembly for each species, by integrating each species-specific repeat database
22 and the Repbase Arthropoda repeat database(Bao et al. 2015) to form the repeats library.

23 We used STAR(Dobin et al. 2013) to do spliced alignments for the RNA sequence from every
24 individual sample. The aligned RNA bam files from all the individual samples for a species were then
25 combined using Samtools. This collective data served as transcriptome hints for predicting genes.

1 We expedited the annotation process by running the BRAKER2(Brúna et al. 2021) ETP mode
2 pipeline independently on each repeat-masked chromosome for each species in parallel. This process
3 involved the use of the aligned species RNA bam file and the NCBI *S. dumicola* protein sequence as
4 the transcriptome evidence and protein homology evidence respectively. The annotations derived
5 from each chromosome were then assembled and merged into a single annotation file in the gff3
6 format for each species. Lastly, we used BUSCO(Simão et al. 2015) to gauge the completeness of the
7 genome annotations, employing the Arthropoda ortholog database for this purpose.

8 The above annotation pipeline was completed for the majority of the chromosomes in all species, with
9 two exceptions where the BRAKER2 pipeline using ETP mode failed to annotate the local part of the
10 genome. The HiC_scaffold_11 (dum_8) of *S. dumicola* is annotated with the BRAKER2 with only
11 RNA transcriptome data as the evidence. For the ending half of HiC_scaffold_16 (mim_6) of *S.*
12 *mimosarum*, we used blat to search for *S. bicolor* mRNA sequence against the part of the genome
13 sequence missing annotations. The hits of the blat search were further parsed as the hints for
14 AUGUSTUS gene prediction. The results from AUGUSTUS gene prediction were combined with the
15 results from BRAKER2 ETP mode.

16 **Incorporation of species without chromosome-level assembly**

17 We do not have the genome assembled from *S. africanus*. To include *S. africanus* in the analyses, we
18 downloaded the transcriptome data of *S. africanus* from Bechsgaard et.al 2019 (Bechsgaard et al.
19 2019) and used Trinity (Haas et al. 2013) to assemble transcripts. We used DIAMOND(Buchfink et
20 al. 2021) blastx mode to align the transcripts to the database of all the translated amino acid sequences
21 from the 10065 single-copy orthologous groups of all six species. 5590 out of 10065 single-copy
22 orthologous groups find one or more hits from the Trinity transcriptome assemblies. We further check
23 the aligned percentage of the hitted orthologous genes and filtered for a percentage of 75% to consider
24 a transcript from *S. africanus* being a valid match to a certain single-copy ortholog groups identified,
25 which ended up with 2649 single-copy orthologous groups.

26

1 We also do not have a genome assembled from *S. pacificus*. To include *S. pacificus* genes into the
2 2649 single-copy orthologous groups identified, we first used BWA-MEM2 (Vasimuddin et al. 2019)
3 to aligned short-read DNA sequence from a *S. pacificus* individual to the *S. sarasinorum* reference
4 genome, which is the closest sister species of it. Then we used SAMtools (Danecek et al. 2021)
5 consensus to call the consensus sequence as the genome of *S. pacificus* based on the BAM file. The
6 sequences of 2649 ortholog genes in *S. pacificus* are then retrieved using the genome annotation file of
7 *S. sarasinorum*. This process can be challenging when there are indels found in *S. pacificus* compared
8 to *S. sarasinorum* reference when we construct the consensus sequence of *S. pacificus*. The sequence
9 of *S. pacificus* and *S. sarasinorum* will not be in alignment as they have different total lengths with
10 different genome coordinate systems. In practice, we fill gaps for deletions and remove insertions in
11 *S. pacificus* based on the reference of *S. sarasinorum* when we construct the consensus sequences.
12 This practice is achieved by setting parameters for SAMtools being "consensus --show-del yes --
13 show-ins no". By ignoring the indels in such a way, we maintain the same coordinate systems
14 between the *S. pacificus* and *S. sarasinorum*. Orthologous sequences in *S. pacificus* can be then
15 retrieved directly using the genome annotation file of *S. sarasinorum* to build multiple sequence
16 alignments across all 8 species for d_N/d_S estimations.

17

18 **Sex Chromosome Identification**

19 We used bwa-mem2 to align reads from a single male individual to the reference genome for each
20 species with a genome assembled. The read depth at each position, covered by at least one read, was
21 obtained using samtools depth. Subsequently, the depth distribution across each scaffolded
22 chromosome was visualized. Chromosomes exhibiting a relative depth in mean and median of half
23 compared to others were identified as X Chromosomes, as detailed in Figure S8.

24

25 **Genome Quality Control**

26 To assess genome quality, we employ Mercury, which measures k-mer completeness and base pair
27 accuracy. In the case of subsocial species, where we successfully reconstruct both haplotypes,
28 Merqury's metrics are provided for the diploid genome assembly. Conversely, for social species

1 characterized by extensive inbreeding, leading to the acquisition of a single haplotype, Merqury's
 2 metrics are presented exclusively for the haploid assembly.

3 Section 3 - d_N/d_S ratio estimations

4 **Estimating the social transition time using intensity of selection**

5 The selection efficiency is expected to be relaxed after social transitions as multiple traits
 6 (reproductive skew, female biased sex ratio, inbreeding) acts to reduce N_e and elevate effects of drift.
 7 Phylogenetic methods (Such as PAML in this study) provide d_N/d_S estimation as a single value per
 8 lineage (shown in Figure 2.D). The single d_N/d_S value for the social lineages thus becomes a weighted
 9 mean of varying selection efficiency through time. We simplify the scenario of selection efficiency
 10 change as a single instant of social transition with a lower d_N/d_S before and a higher d_N/d_S after
 11 (Figure M1). Once knowing the weighted d_N/d_S across whole lineages and the two d_N/d_S values before
 12 and after the transition, the time fraction of the social period can be derived.

13

14 As it is challenging to estimate the d_N/d_S before and after the social transition in social lineages
 15 directly, we use approximations. We use the d_N/d_S from the subsocial sister species of each social
 16 species as the approximation for d_N/d_S before the social transition and p_{iN}/p_{iS} between isolated
 17 populations of social species as the approximation for d_N/d_S after the social transition ("social d_N/d_S ").

18

19 **Benchmarking for substitution of "social d_N/d_S " with p_{iN}/p_{iS} across social species populations**

20 The general application of d_N/d_S aims to test the selection strength by investigating the fixed non-
 21 synonymous and synonymous substitutions between species. We used p_{iN}/p_{iS} between divergent
 22 populations of the same species as an approximation of "social d_N/d_S ". This implication has a risk of
 23 overestimating the d_N/d_S . As d_N/d_S compares the fixed nucleotide difference between species under
 24 certain selection strength, while p_{iN}/p_{iS} includes the nucleotide differences that are not fixed by
 25 selection yet. Thus, the sites included in the p_{iN}/p_{iS} would likely contain more deleterious non-
 26 synonymous mutations that are not removed by selection, which leads to an overestimated d_N/d_S . The

1 overestimation could happen if the selection strength on the non-synonymous sites are much higher
 2 than the selection strength on synonymous sites, which result in a higher observed p_{iN}/p_{iS} than the
 3 actual d_N/d_S after fixation.

4

5 First, we benchmarked the reliability of this substitution strategy by comparing the site frequency
 6 spectrum of non-synonymous and synonymous sites in an *S. dumicola* population, which has the
 7 shortest population divergent time with potentially more polymorphisms unfixed between
 8 populations. We called genotypes for 9 individuals from *S. dumicola* using the GATK pipeline and
 9 filtered for bi-allelic single nucleotide variants where the genotype quality is over 30. We used snpEff
 10 (version 5.2) (Cingolani et al. 2012) to build a database with our de novo assemblies and annotations
 11 and classify variants as either missense variants or synonymous variants. After the classification, the
 12 site frequency spectrum was built for missense variants and synonymous variants respectively (Figure
 13 S7). The high similarity of N-sites spectrum and S-sites spectrum suggest the ongoing selection acting
 14 similarly on N-sites and S-sites, countering the concern that selection is more effective in removing
 15 polymorphism in N-sites than S-sites.

16

17 Second, we evaluate whether there are substantial amounts of deleterious polymorphisms segregating
 18 in the social species leading to over estimation of d_N/d_S by using p_{iN}/p_{iS} . We assume that deleterious
 19 mutations that can be removed by selection are less likely to segregate within the population. We then
 20 quantify the fraction of common variants out of the polymorphisms we identified between the two
 21 individuals selected from separate populations. We have 20 individuals (40 alleles per site, 10
 22 individuals from each population) from *S. dumicola* and 15 individuals (30 alleles per site, 8
 23 individuals from Madagascar and 7 individuals from mainland Africa) from *S. mimosarum*. We
 24 assume different minimum thresholds based on minor allele count (2 to 10) we found in each species
 25 to filter for “common variants” (See result in Table S5). With a conservative filter that the minor
 26 allele count has to be greater or equal than 10, common variants compose 66.43% of polymorphisms
 27 used for p_{iN}/p_{iS} estimation of *S. dumicola* are 91.52% of polymorphisms used for p_{iN}/p_{iS} estimation of
 28 *S. mimosarum*. The high fraction of common alleles of the used polymorphisms for p_{iN}/p_{iS} estimation

1 also support that there is only a small proportion of segregating deleterious mutations that can lead to
 2 overestimation of “social d_N/d_S ”.

3

4 In the end, we select the polymorphisms that are fixed differently between the two isolated
 5 populations used for cross-population p_{iN}/p_{iS} estimations. We find that 17.60% of polymorphisms are
 6 fixed in *S. dumicola* and 74.34% of polymorphisms are fixed in *S. mimosarum* (Table S6). We then
 7 estimate “social d_N/d_S ” using only fixed polymorphism across populations, which would be expected
 8 to reflect the true selection efficiency free from unremoved deleterious segregating sites. We find the
 9 point estimation of “social d_N/d_S ” for *S. mimosarum* is 0.2990 using fixed polymorphisms compared
 10 to previous estimation of 0.3043 using polymorphic sites between two individuals (Figure S12). And
 11 the new “social d_N/d_S ” estimation for *S. dumicola* is 0.3558 compared to previous estimation of
 12 0.3366. The high similarity between the two estimations quantifies the potential bias to overestimate
 13 “social d_N/d_S ” is arguably neglectable in *S. mimosarum* and *S. dumicola*.

14

15 We do not have more individuals to create population sets for Himalayas population and Sri Lanka
 16 population of *S. sarasinorum*. Thus, no empirical benchmarking has been done for *S. sarasinorum*.
 17 However, population divergence time is longer for *S. sarasinorum* (110 kya) compared to *S. dumicola*
 18 (20kya), indicating the concern for overestimation would not be larger than for *S. dumicola*.

19

20 **Coding gene sequence alignment and filtering for d_N/d_S estimation**

21 For getting reliable alignments for d_N/d_S estimation, we made a strict and conserved filtering for
 22 ortholog groups. We ended up analyzing 2302 autosomal genes and 347 single-copy ortholog groups
 23 across the 8 species. After retrieving the nucleotide sequence from all species of each ortholog group,
 24 we did the alignment using MACSE alignSequences to account for potential frameshift since we are
 25 aligning coding sequences(Ranwez et al. 2018). With MACSE, we ensured that the alignment of each
 26 single-copy ortholog is always a multiple of 3 in length.

27

1 We do resampling estimation of d_N/d_S for X Chromosomes and autosomes separately. We randomly
2 sample 500 or 100 ortholog groups out of the 2302 autosomal genes or 347 X Chromosome genes
3 respectively. The random sample was repeated 500 times for autosomal genes and 100 times for X
4 Chromosome genes to get standard error of the mean estimation. For each sampled set of genes, we
5 concatenated the alignment using GoAlign(Lemoine and Gascuel 2021). We then checked for the
6 concatenated alignment for every codon which contains gaps in any of the species, any codon with
7 gaps in alignment will be marked as removed. The codon marked as removed further divided the
8 whole alignment into continuous alignment blocks in different sizes. An overall distribution of the
9 polymorphic site fraction and alignment block size (Figure S2) suggest that a small size of alignment
10 block with high polymorphic fraction represents local mis-alignment in general. Hence, we filter for
11 alignment blocks that are at least 300 continuous nucleotides long and the fraction of polymorphic
12 sites in a local alignment block should be less than 15%. The above filter was conserved and might
13 lead to fewer sites in final d_N/d_S estimation, which can be compensated with the concatenation
14 process, but should be more robust to be free from mis-alignment.

15

16 **Resampling strategy for quantifying confidence interval of d_N/d_S estimations**

17 The choice of "sampling 500 times of 500 genes out of 2302 autosomal genes without replacement"
18 is relatively arbitrary and aiming for a reasonable estimation for getting variation estimates for our
19 genome-wide selection intensity (d_N/d_S) estimations. If we choose too many genes, for example 2000,
20 then each run of the resampling without replacement will be similar, which may not reflect the true
21 variance in the genome-wide selection intensity estimation, because data between resampling runs are
22 expected to be highly overlapping. Meanwhile, we aim for a "genome-wide" selection intensity
23 estimate, which requires a substantial amount of genes. Otherwise, gene-specific selection intensity
24 contributes to higher noise. That is why we arbitrarily choose 500 genes, which should not result in a
25 high overlapping rate between resampled data sets but still be able to reflect a genome-wide signal.
26 We show that 500 rounds of resampling already reveal a normal distribution of estimated genome-
27 wide selection intensity (Figure S10). It is also worth noting that the resampling here requires

1 substantial computation resources as each round requires a resampling of the raw sequence data, thus
 2 we limited the number of rounds to what we regard a sufficient amount.
 3
 4 To get a confidence interval of estimated social transition time, we performed 10000 rounds of
 5 calculation for social transition times. The calculation of social transition time need four values,
 6 which are the d_N/d_S on the social lineage, the d_N/d_S on the subsocial sister species lineage, and the
 7 p_{iN}/p_{iS} from the isolated populations of social species, and the dS branch length of the social lineage.
 8 All the four values have a confidence interval estimated from the previous resampling process
 9 (500*500). To account for the influence of uncertainty of selection intensity and species divergence
 10 time on our estimation of social transition, we sampled four values 10000 times from each their
 11 distribution (built based on the 500*500 resamples), which allow us to explore the confidence interval
 12 of social transition times. This final resampling process is less computational intensive since we only
 13 need to sample values from a known distribution, which allows us to do it as many times as needed.

14
 15 **Testing for relaxed selection**

16 We use RELAX from HyPhy (Wertheim et al. 2015) to test for the observed higher d_N/d_S in social
 17 species due to intensification of positive selection or relaxed purifying selection. We used the
 18 concatenated alignment of all autosomes and X Chromosomes separately and 4 different grouping
 19 strategies of testing branches and reference branches. For each social species, we used the social
 20 species branch as the "Test" and the subsocial sister branches and common ancestor branches as the
 21 "Reference". We also have an extra contrasting group where all the social species branches are used
 22 as the "Test" and rest branches in the phylogeny are used as the "Reference".
 23 RELAX classify the sites of a alignment into three categories, thus each category are assigned
 24 with a fraction:

25 a. Sites with d_N/d_S closer to 1. (o2 in Figure S3)
 26 b. Sites with d_N/d_S much larger than 1.(o1 in Figure S3)
 27 c. Sites with d_N/d_S much smaller than 1. (o3 in Figure S3)

1 Then RELAX estimates a d_N/d_S value (shown on x-axis of Figure S3) of sites in each category for
2 reference branches and test branches separately. When relaxed selection dominates the
3 observation of higher d_N/d_S in test branches than reference branches, the d_N/d_S value estimated for
4 test branches in category a and c will be both shifted towards $d_N/d_S = 1$ compared to results of
5 reference branches.

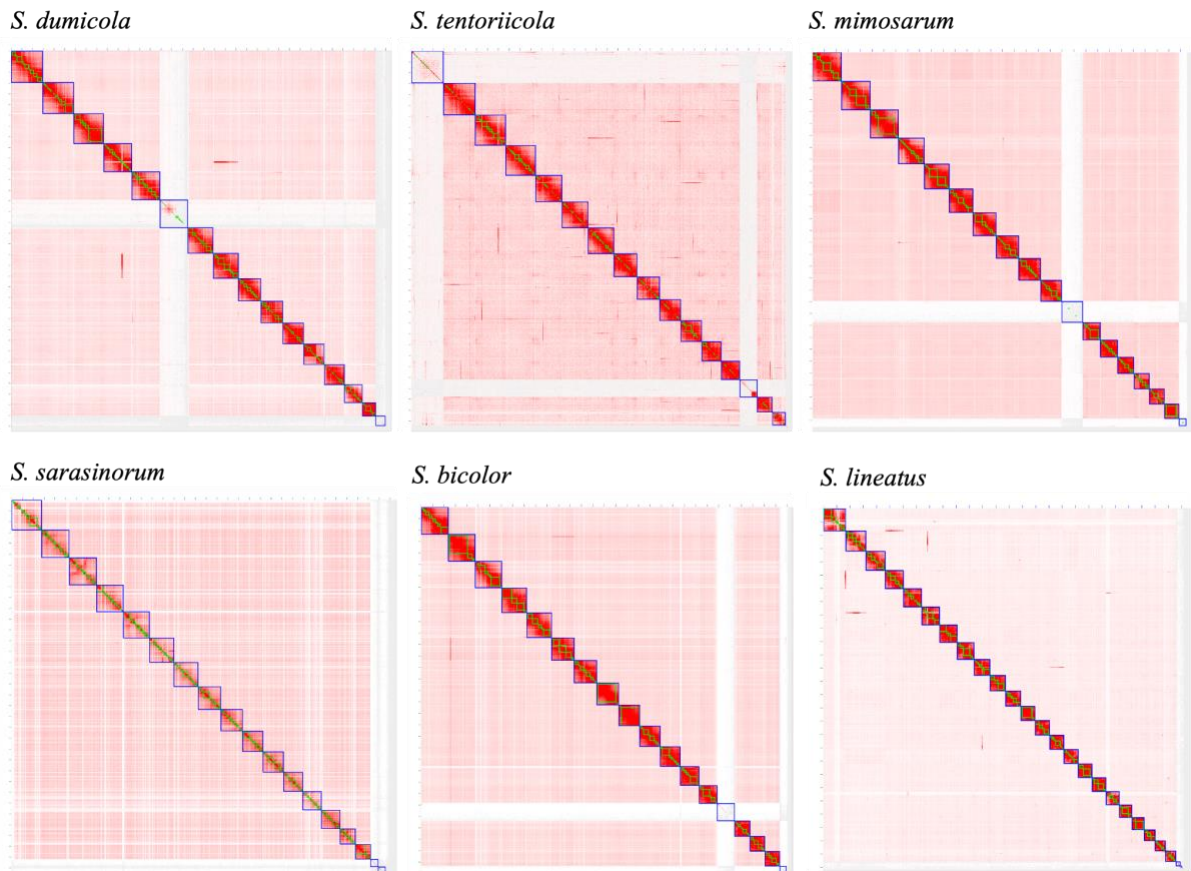
6

7

8

1 Supplementary Figures

2



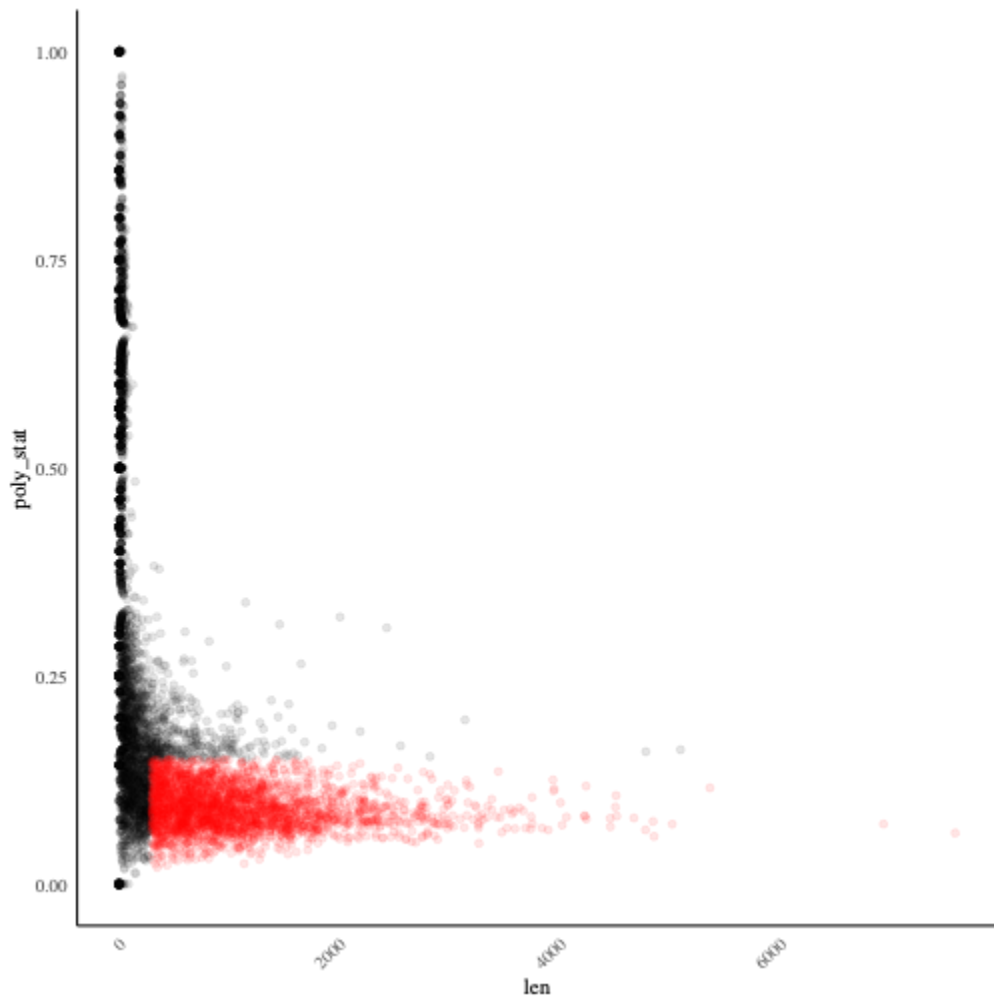
3

4 Figure S1. HiC contact map of genome assemblies. The density of red color denotes the hic contact
 5 density between regions in the assembly. The green box denotes initial contigs assembled from Pacbio
 6 HiFi long reads using hifiasm. The blue box denotes the candidate chromosome-level scaffolds. Each
 7 blue box supported by higher intra-scaffold density of HiC contact pattern compared to inter-scaffold
 8 HiC contact is identified as a chromosome. The blue box without high intra-scaffold density of HiC
 9 contact remains scaffolded.

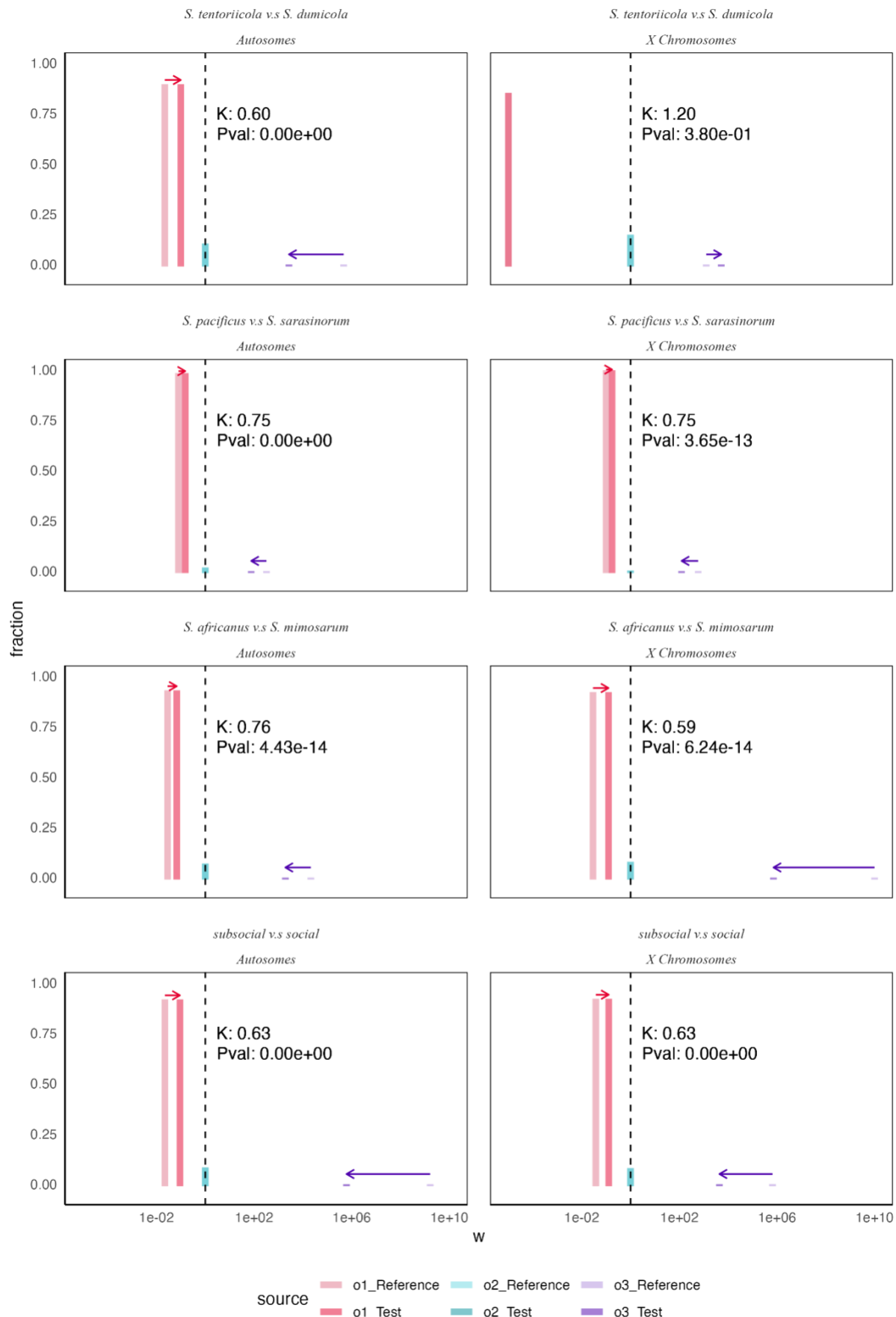
10

11

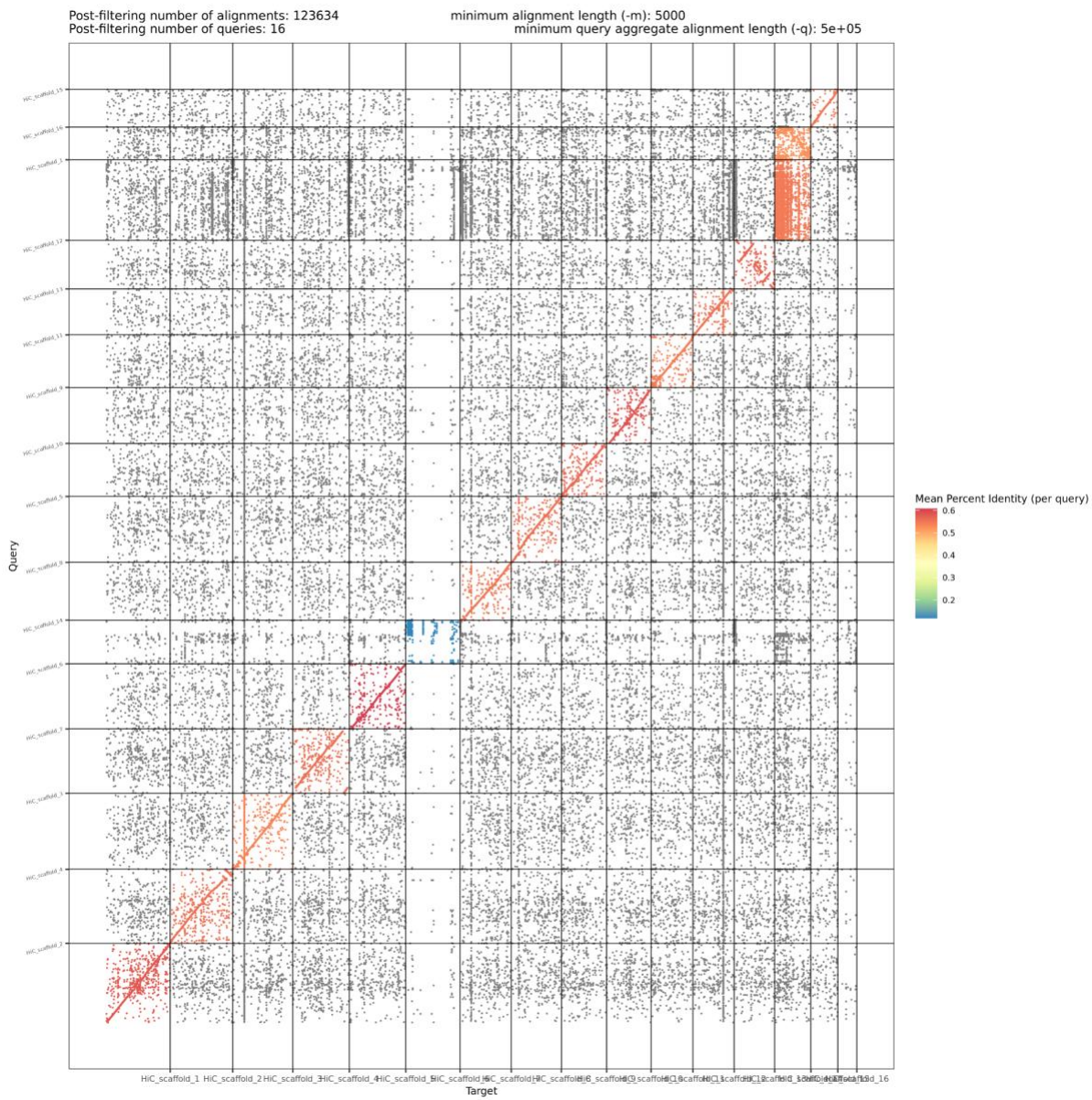
12



1
2 Figure S2 The size of alignment blocks without gaps versus the fraction of polymorphic sites for all
3 alignment blocks of concatenated 2302 autosome gene alignments. The alignment blocks colored in
4 red are further used for estimating d_N/d_S in PAML(Yang 2007).



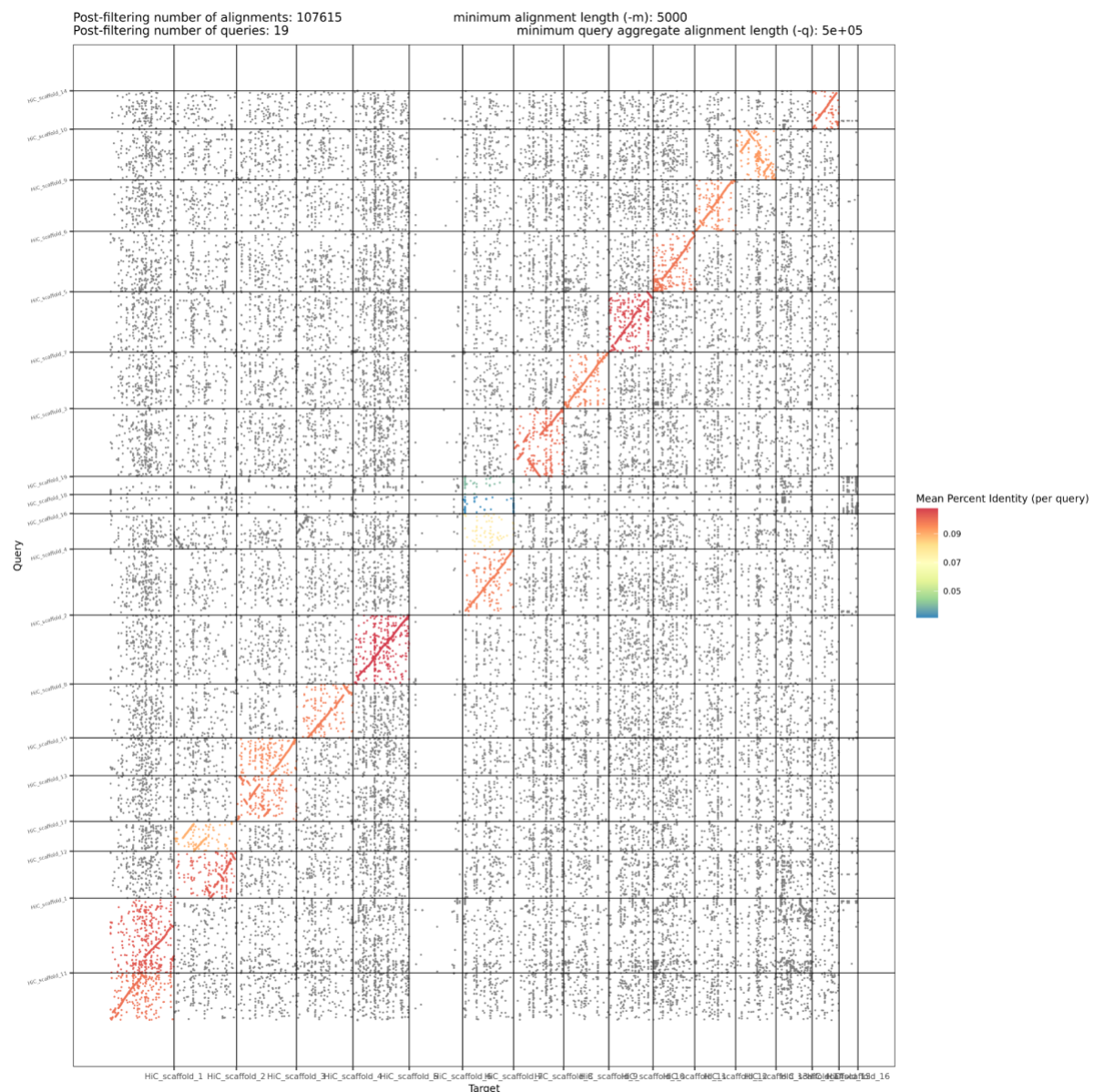
1 Figure S3. RELAX results for different contrasting pairs using genes from autosomes and X
2 Chromosomes separately. The social lineage(s) are always used as the test set and their corresponding
3 sister subsocial lineage(s) are used as the reference set. $K > 1$ implies intensification of positive
4 selection and $K < 1$ implies relaxation of purifying selection. o1 represents the sites that are under
5 strong purifying selection ($w \ll 1$), o2 represents the sites that are close to neutral ($w \approx 1$), o3
6 represents the sites that are under positive selection ($w \gg 1$). The x axis shows estimated w (d_N/d_s)
7 for each category (o1, o2, o3) and the y axis shows the fraction of sites in the genome of the
8 corresponding w categories (o1, o2, o3) for reference branches and test branches respectively. The
9 arrow indicates the shifting direction from reference branches to test branches in the corresponding w
10 category (o1, o2, o3). Relaxed selection in the test branches will be reflected as the shifting direction
11 of arrows points to $w = 1$ (black dashed line) on both sides of the black dashed line.
12



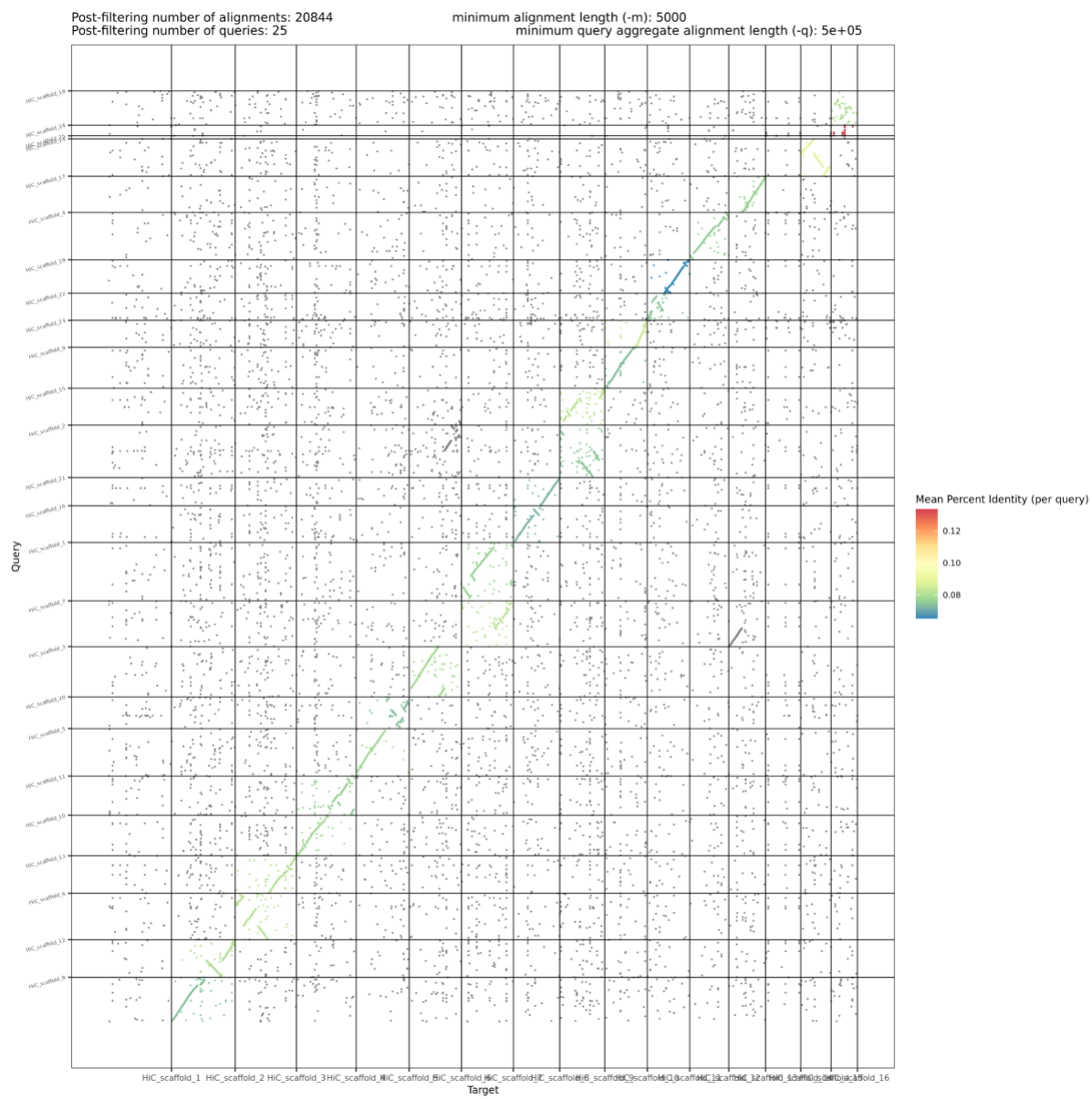
1

2 Figure S4. The dot plot from dotPlotly between genome assemblies of *S. dumicola* (x-axis) and *S.*
 3 *tentoriicola* (y-axis). Each point denotes an alignment length of minimum 5000 base pairs. Percentage
 4 of identity is shown for each comparison group of chromosomes.

5

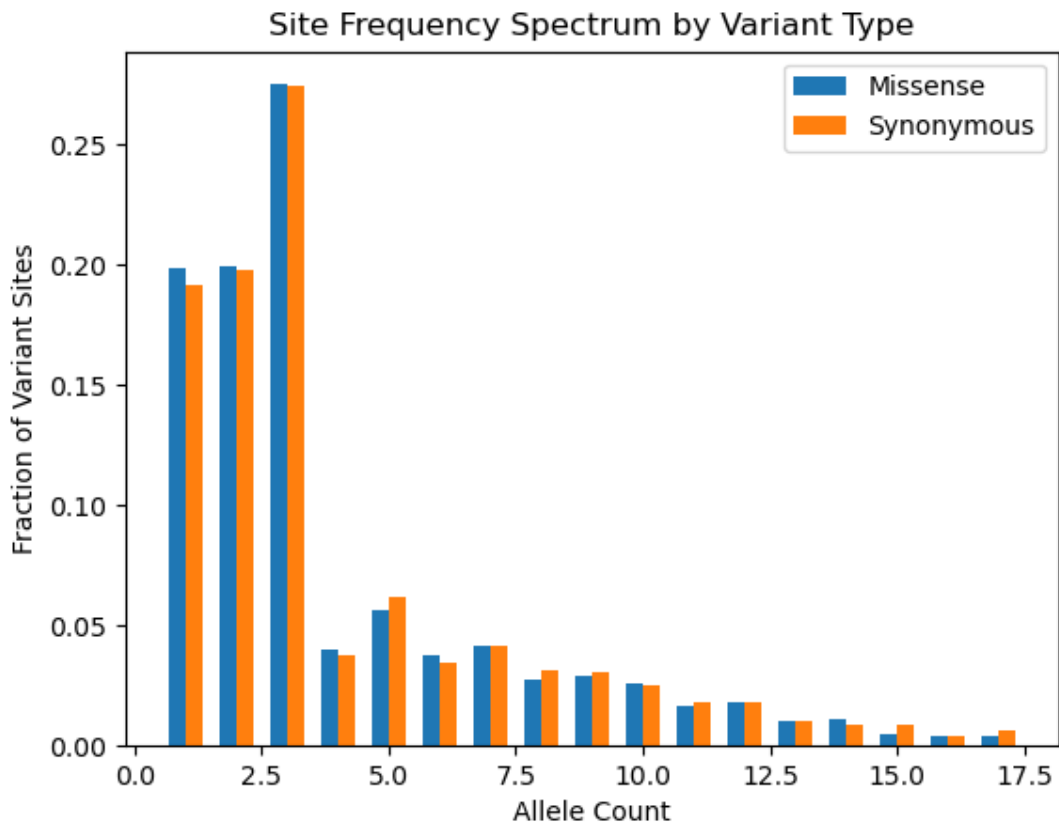


2 Figure S5. The dot plot from dotPlotly between genome assemblies of *S. dumicola* (x-axis) and *S.*
 3 *sarasinorum* (y-axis). Each point denotes an alignment length of minimum 5000 base pairs.
 4 Percentage of identity is shown for each comparison group of chromosomes.
 5



2 Figure S6. The dot plot from dotPlotly between genome assemblies of *S. tentoriicola* (x-axis) and *S.*
 3 *lineatus* (y-axis). Each point denotes an alignment length of minimum 5000 base pairs. Percentage of
 4 identity is shown for each comparison group of chromosomes.

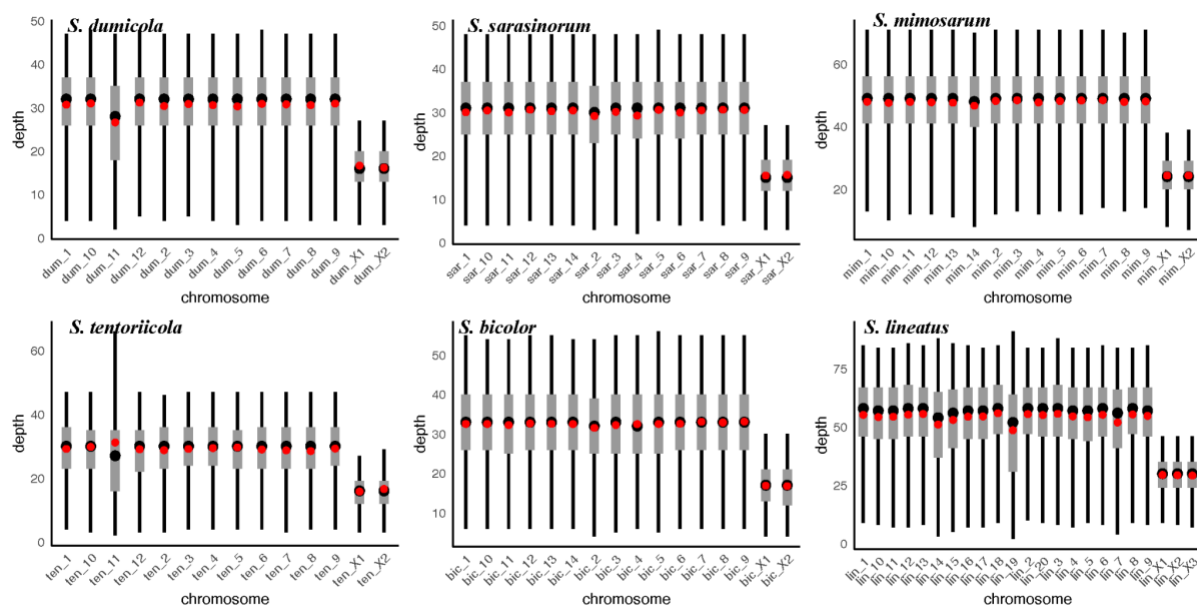
5



1

2 Figure S7. Site frequency spectrums for missense variants and synonymous variants separately based

3 on 9 individuals from *S. dumicola*.



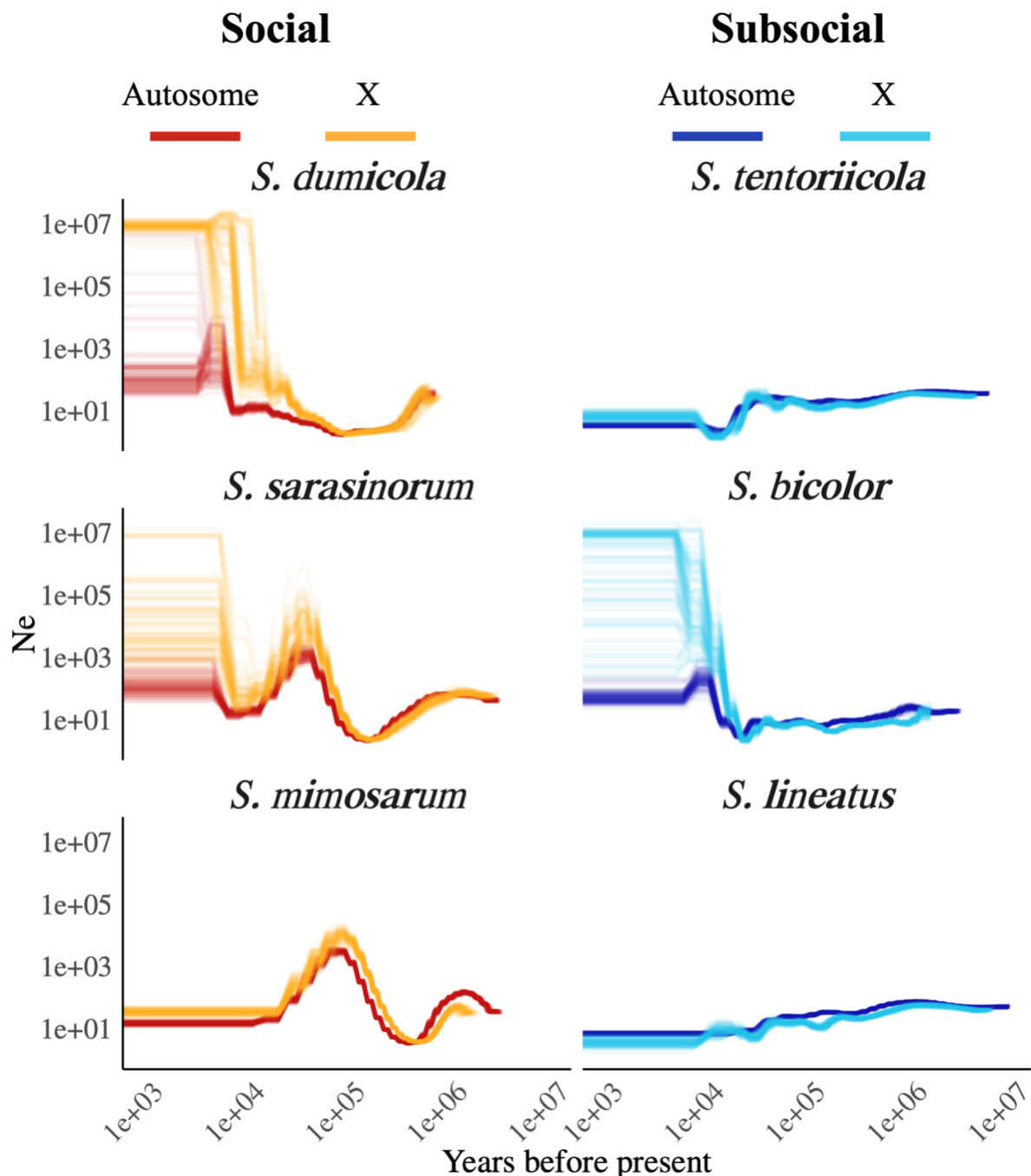
4

5 Figure S8. A boxplot of chromosome-level depth distribution from a single male individual for each

6 species. The black lines mark from quantile 2.5% to quantile 97.5%. The grey boxes mark from

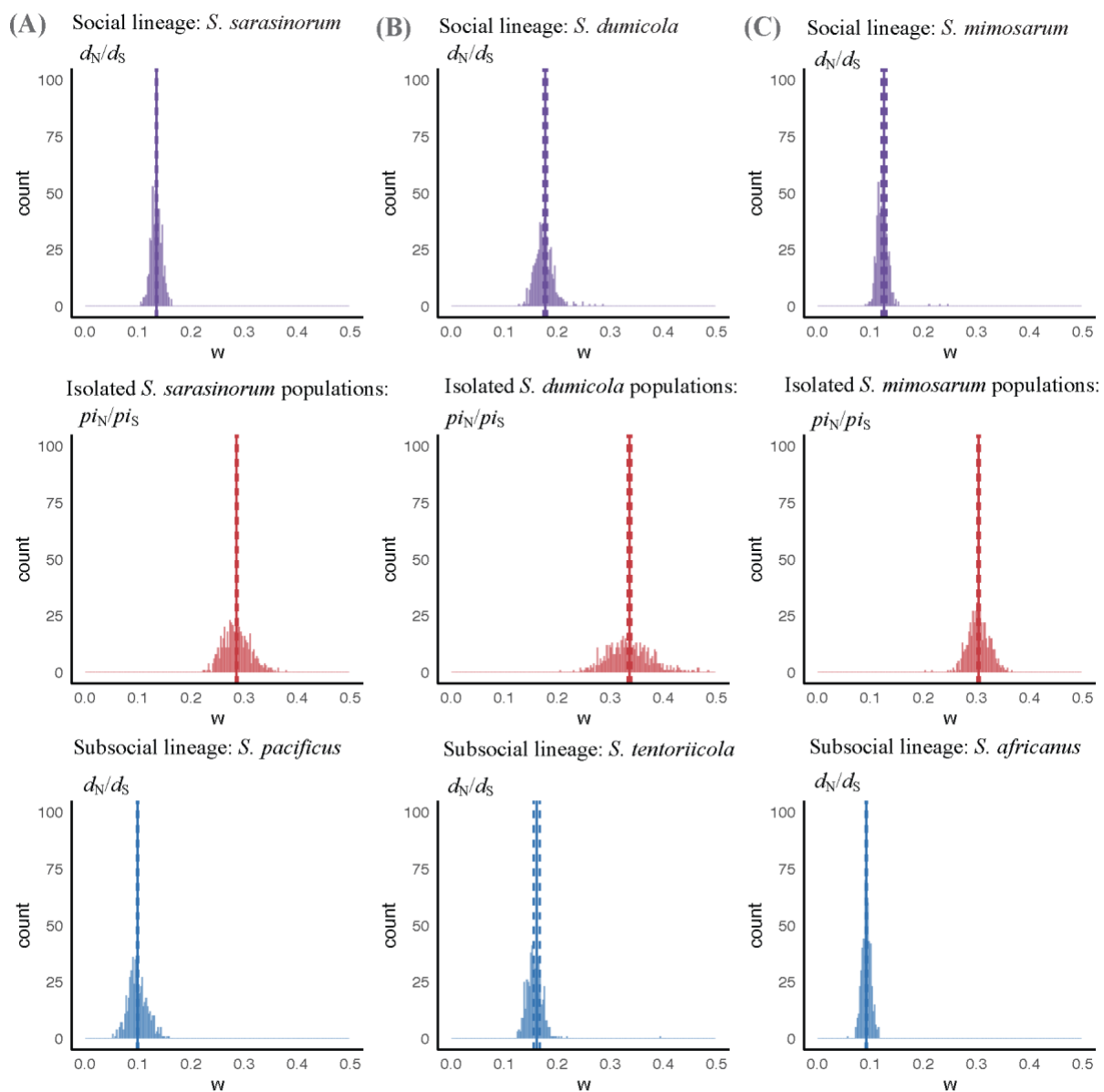
1 quantile 25% to quantile 75%. The black points and red points mark the median depth and mean depth
 2 respectively.

3



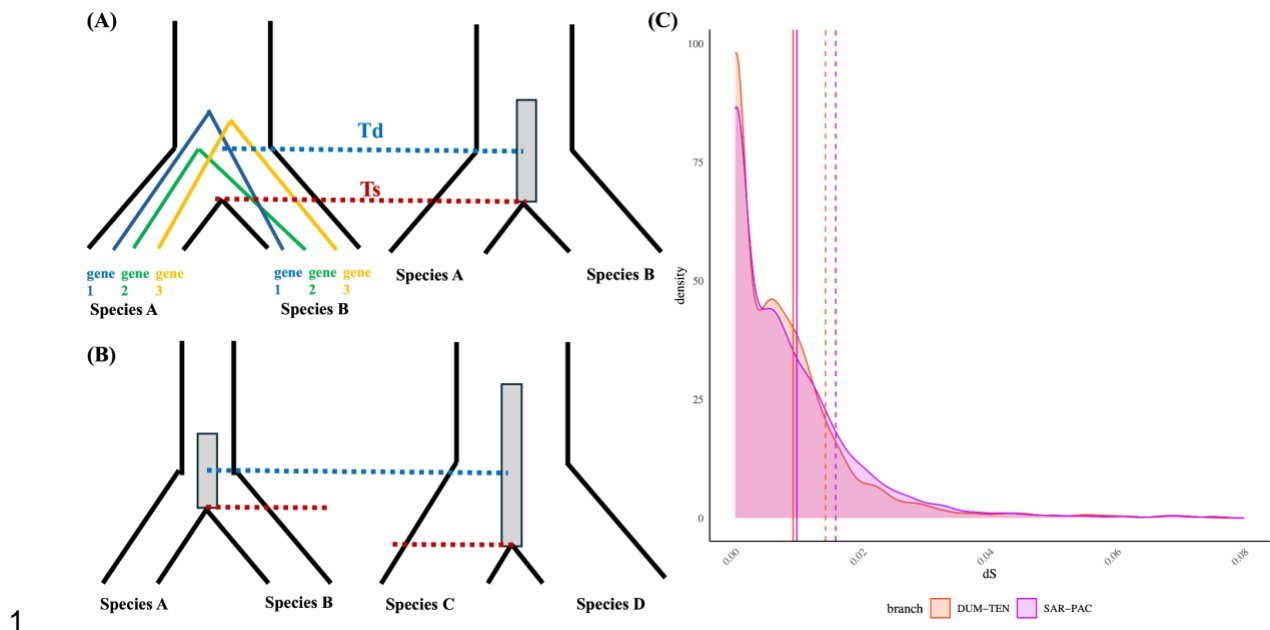
4
 5 Figure S9. The historical effective population size inferred from the Pairwise Sequentially Markovian
 6 Coalescent (PSMC) model with 100 rounds of bootstrapping, setting segment size of 100000bp in
 7 resampling process, for different *Stegodyphus* species with chromosome-level assembly. Results from
 8 autosomes and X Chromosomes are shown separately for each species

1



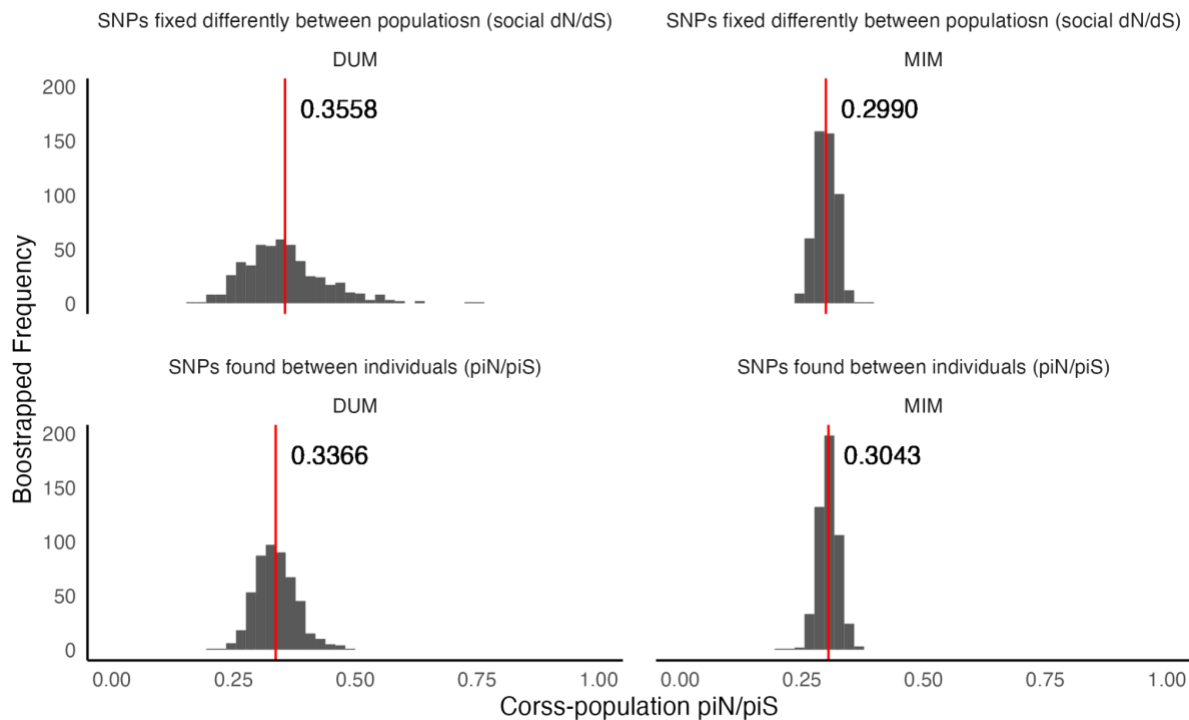
2

3 Figure S10. The distributions of d_N/d_S and π_{iN}/π_{iS} in each species, based on 500 independent
 4 resampling runs, where each run samples random 500 genes out of 2303 autosomal genes without
 5 replacement. The point estimation from the mean and 95% confidence interval of the mean are
 6 denoted by vertical lines in solid lines and dash lines respectively.



1 Figure S11. Coalescence expectations of distance between species divergence time (Td) and
2 speciation time (Ts) for *S. dumicola* and *S. sarasinorum*. (A) Different ortholog genes can coalesce at
3 different time points between a pair of species. This provides a time interval on average of $2Ne$
4 generations for a gene to coalesce in the ancestral populations, which is the distance between species
5 divergence time (Td) and speciation time (Ts) (from the speciation to the middle point of the grey
6 box). (B) Difference in expected coalescence time between Td and Ts for different ancestral
7 population size. The species pair of species A and species B has a smaller ancestral Ne than the pair
8 of species C and species D. (C) Distribution of dS from each autosomal ortholog gene (2303 in total)
9 for *S. dumicola* (red) and *S. sarasinorum* (pink). The solid vertical lines are the median of the dS
10 distributions, which is expected to correlate with Td (blue dashed line) in (A) and (B). The dashed
11 vertical lines are the 75% quantile of the dS distributions. The distance between the solid vertical line
12 and dashed vertical line in each species is expected to correlate with the width of the distribution,
13 which represents the height of the grey box illustrated in (B).

15



1 Figure S12. Benchmarking for using π_N/π_S as an approximation of “social d_N/d_S ” in *S. dumicola* and
 2 *S. mimosarum*. The distribution shows the bootstrap π_N/π_S estimations of two different subsets of
 3 SNPs. 1. We filtered SNPs to analyse only polymorphic sites between an individual from two isolated
 4 populations (bottom graphs, π_N/π_S shown in Figure 4 and Figure 5) and 2. Using population data, we
 5 further filtered SNPs to keep only polymorphic sites fixed differently between two populations
 6 (upper graph, “social d_N/d_S ”). The point estimation is shown as the vertical red lines and marked with
 7 text.
 8

9 Supplementary Reference

10

11 Bao W, Kojima KK, Kohany O. 2015. Repbase Update, a database of repetitive elements in
 12 eukaryotic genomes. *Mob DNA* **6**: 11.

13 Bechsgaard J, Schou MF, Vanthournout B, Hendrickx F, Knudsen B, Settepani V, Schierup MH,
 14 Bilde T. 2019. Evidence for Faster X Chromosome Evolution in Spiders. *Mol Biol Evol* **36**:
 15 1281–1293.

16 Brúna T, Hoff KJ, Lomsadze A, Stanke M, Borodovsky M. 2021. BRAKER2: automatic eukaryotic
 17 genome annotation with GeneMark-EP+ and AUGUSTUS supported by a protein database. *NAR*
 18 *Genom Bioinform* **3**: lqaa108.

19 Buchfink B, Reuter K, Drost H-G. 2021. Sensitive protein alignments at tree-of-life scale using

1 DIAMOND. *Nat Methods* **18**: 366–368.

2 Cheng H, Concepcion GT, Feng X, Zhang H, Li H. 2021. Haplotype-resolved de novo assembly using
3 phased assembly graphs with hifiasm. *Nat Methods* **18**: 170–175.

4 Cingolani P, Platts A, Wang LL, Coon M, Nguyen T, Wang L, Land SJ, Lu X, Ruden DM. 2012. A
5 program for annotating and predicting the effects of single nucleotide polymorphisms, SnpEff:
6 SNPs in the genome of *Drosophila melanogaster* strain w1118; iso-2; iso-3. *Fly* **6**: 80–92.

7 Danecek P, Bonfield JK, Liddle J, Marshall J, Ohan V, Pollard MO, Whitwham A, Keane T,
8 McCarthy SA, Davies RM, et al. 2021. Twelve years of SAMtools and BCFtools. *Gigascience*
9 **10**. <http://dx.doi.org/10.1093/gigascience/giab008>.

10 Dobin A, Davis CA, Schlesinger F, Drenkow J, Zaleski C, Jha S, Batut P, Chaisson M, Gingeras TR.
11 2013. STAR: ultrafast universal RNA-seq aligner. *Bioinformatics* **29**: 15–21.

12 Dudchenko O, Batra SS, Omer AD, Nyquist SK, Hoeger M, Durand NC, Shamim MS, Machol I,
13 Lander ES, Aiden AP, et al. 2017. De novo assembly of the *Aedes aegypti* genome using Hi-C
14 yields chromosome-length scaffolds. *Science* **356**: 92–95.

15 Durand NC, Robinson JT, Shamim MS, Machol I, Mesirov JP, Lander ES, Aiden EL. 2016. Juicebox
16 Provides a Visualization System for Hi-C Contact Maps with Unlimited Zoom. *Cell Syst* **3**: 99–
17 101.

18 Flynn JM, Hubley R, Goubert C, Rosen J, Clark AG, Feschotte C, Smit AF. 2020. RepeatModeler2
19 for automated genomic discovery of transposable element families. *Proc Natl Acad Sci U S A*
20 **117**: 9451–9457.

21 Haas BJ, Papanicolaou A, Yassour M, Grabherr M, Blood PD, Bowden J, Couger MB, Eccles D, Li
22 B, Lieber M, et al. 2013. De novo transcript sequence reconstruction from RNA-seq using the
23 Trinity platform for reference generation and analysis. *Nat Protoc* **8**: 1494–1512.

24 Lemoine F, Gascuel O. 2021. Gotree/Goalign: toolkit and Go API to facilitate the development of
25 phylogenetic workflows. *NAR Genom Bioinform* **3**: lqab075.

26 Ranwez V, Douzery EJP, Cambon C, Chantret N, Delsuc F. 2018. MACSE v2: Toolkit for the
27 Alignment of Coding Sequences Accounting for Frameshifts and Stop Codons. *Mol Biol Evol*
28 **35**: 2582–2584.

29 Settepani V, Bechsgaard J, Bilde T. 2014. Low genetic diversity and strong but shallow population
30 differentiation suggests genetic homogenization by metapopulation dynamics in a social spider.
31 *J Evol Biol* **27**: 2850–2855.

32 Simão FA, Waterhouse RM, Ioannidis P, Kriventseva EV, Zdobnov EM. 2015. BUSCO: assessing
33 genome assembly and annotation completeness with single-copy orthologs. *Bioinformatics* **31**:
34 3210–3212.

35 Tarailo-Graovac M, Chen N. 2009. Using RepeatMasker to identify repetitive elements in genomic
36 sequences. *Curr Protoc Bioinformatics* **Chapter 4**: 4.10.1–4.10.14.

37 Vasimuddin M, Misra S, Li H, Aluru S. 2019. Efficient Architecture-Aware Acceleration of BWA-
38 MEM for Multicore Systems. In *2019 IEEE International Parallel and Distributed Processing*
39 *Symposium (IPDPS)*, pp. 314–324.

40 Wertheim JO, Murrell B, Smith MD, Kosakovsky Pond SL, Scheffler K. 2015. RELAX: detecting

1 relaxed selection in a phylogenetic framework. *Mol Biol Evol* **32**: 820–832.

2 Yang Z. 2007. PAML 4: phylogenetic analysis by maximum likelihood. *Mol Biol Evol* **24**: 1586–
3 1591.

4